ISSN: 0976-3031

Available Online at http://www.recentscientific.com

CODEN: IJRSFP (USA)

International Journal of Recent Scientific Research
Vol. 10, Issue, 07(G), pp. 33763-33767, July, 2019

International Journal of Recent Scientific Research

DOI: 10.24327/IJRSR

Research Article

SYNTHESIS AND CHARACTERIZATION OF SULFUR DOPED TiO² NANOPARTICLES FOR THE IMPROVED PHOTOCATALYTIC DEGRADATION OF RHODAMINE B BY SOL-GEL ROUTE

Kavitha V

Department of Physics, Adhiyaman Arts & Science College for women, Uthangarai, Tamil nadu

DOI: http://dx.doi.org/10.24327/ijrsr.2019.1007.3744

ARTICLE INFO

Article History:

Received 13th April, 2019
Received in revised form 11th May, 2019
Accepted 8th June, 2019
Published online 28th July, 2019

Key Words:

TiO_2 nanoparticle, Solgel method, Photocatalytic activity, Rhodamine.

ABSTRACT

Nanocrystalline TiO_2 sample has been synthesized by using Titanium (IV) isopropoxide and sodium sulfate as precursors via an simplistic route called sol-gel synthesis at 500°C temperatures. The synthesized products were characterized by XRD, Fourier transform infrared spectroscopy (FT-IR), Scanning electron microscopy (SEM/EDS), transmission electron microscopy (TEM), UV-Visible spectroscopy (UV-Vis) and Photoluminescence spectroscopy (PL). The sulfur concentration increased the crystallization of TiO_2 from anatase to rutile. The analysis confirmed that the TiO_2 nano crystals are below 30 nm. The presence of functional groups and chemical bonding is confirmed by FTIR. The morphology of TiO_2 powders was of irregular shape nanoparticles with various caves, which mainly resulted from the agglomeration of nanocrystaline TiO_2. The PL performed the UV emission peak in a range of 430-470 nm with red shift.

INTRODUCTION

In current years, semiconductor mediated photocatalytic treatment of organic pollutants has established much attention. After the finding of photo electrochemical splitting of water on titanium dioxide TiO_2 electrodes [1], semiconductor- based photocatalysis has received a lot of attention [2,3]. Many other significant uses have also been studied, particularly in the medical and biological fields, where TiO_2-based nanomaterials have been explored for in cancer therapy [5], vivo imaging [4], protein separation purification, and as bactericides [6]. These applications exploit TiO_2 across a broad range of sizes from hundreds of nanometers to several micrometers. Even though these applications account for the greater part of global TiO_2 consumption, its consumption in nanoscale research has mainly focused on it's in the vicinity of semiconductor photocatalytic properties. TiO_2 has showed to be an excellent catalyst in the photocatalytic degradation of organic pollutants since it is effective, photostable, non-toxic and easily available [7]. TiO_2 n-type semiconductor consists of three polymorphs (rutile, anatase, and brookite), and is a large amount widely applied heterogeneous photocatalyst for environmental pollutant treatment due to its oxidation capacity, thermal and chemical stability, and low cost [8, 9]. Two major factors govern the photocatalytic activity of TiO_2: lowering of band gap energy in visible region & prevention of electron hole recombination rate. One of the methods to get better photocatalytic activity of TiO_2 is to add non-metal or metal impurity in the TiO_2 lattice or to couple with lower band gap semiconductor [10, 11].

Most of these explorations have been carried out under ultraviolet (UV) light, because TiO_2 photocatalyst explains relatively high activity and chemical stability under UV light, which exceed the band-gap energy of 3.0 or 3.2 eV in the rutile crystalline phase, respectively. Thus TiO_2 cannot be making active in visible light or sunlight. Doping is one of the distinctive approaches to extend the spectral reply of a wide band gap semiconductor to visible light, where several metal ions can be used as a dopant [12]. Still, photocatalytic activity of most of these catalysts decreases even in the UV region, since the doped materials endure from a thermal instability or an increase in the carrier-recombination centers [13].

A variety of approaches have been made in the bid to delay recombination of the photogenerated electron-hole pairs in nano-TiO_2. Nonmetal doping has been thoroughly investigated since the electronic states of nonmetals are above the valence band edge of TiO_2 compared with pure TiO_2. Consequently, different nonmetal dopants including nitrogen (N), carbon (C), and sulfur (S) have been tested for their capability to improve the morphology and photocatalytic performance of TiO_2 [14,

Corresponding author:* **Kavitha V
Department of Physics, Adhiyaman Arts & Science College for women, Uthangarai, Tamil nadu

15]. The presence of nonmetal anions increases the percentage of the rutile phase in TiO_2, restrains the growth of crystallite size of TiO_2, and increases the specific surface area of TiO_2 [16]. In this direction, sulfur doping is descripted to be beneficial for rising highly efficient titania that is responsive below wide spectral range. The substitution of sulfur in either cationic or anionic sites depends on the experimental conditions as well as on the choice of precursor. The sulfur replaces Ti^{4+} ions in TiO_2 lattice in both anatase and rutile phases; additional it reduces the band gap absorption energy [17].

In the present study, the most convenient ways of synthesizing various nanomaterials are preferable due to low cost, ease fabrication and low temperature. This method has various advantages over other methods, such as co-precipation or allowing impregnation, which can be achieved by introducing dopant, molecular scale mixing, high purity of the precursors and homogeneity of sol-gel products with high purity physical, morphological and chemical properties of nanomaterial. Consequently, that was the reason why sol gel synthesis method is chosen as the method of titanium dioxide nanomaterials.

Rhodamine B is a dye that belong to a class of compounds called xanthenes, with a Mol. Wt.479.02 $gmol^{-1}$ and a formula $C_{28}H_{31}N_{20}O_3Cl$. It is expansively used as model compound since it shows a strong absorption band in the visible region of the electromagnetic spectrum (555 nm) [18]. Now this dye has been forbidden for the use as food color because it is suspected that RhB could be a carcinogenic substance [19, 20], inducing mutagenesis and teratogenesis in rats [21]. Their stability, resistance to biological & chemical degradation, presence in textile industry effluents, and it was suspected that this dye could be a possible carcinogenic substance, implies that Rhodamine B is an excellent model compound for this type of study.

Experimantal

Materials

All chemicals were in analytical grade and were used as received without any additional purification. Titanium (IV) isopropoxide, ($C_{12}H_{28}O_4Ti$, purity 97% Aldrich) was used as starting precursor for synthesizing crystalline TiO_2 particles, sodium sulfate $Na_2SO_4.5H_2O$ as a dopant precursor, and nitric acid obtained from Hi-media. Deionized water was employed throughout the experiments.

Synthesis

5 ml Titanium tetra isopropoxide (TTIP) was dissolved with 20 ml of isopropanol. This solution was added dropwise to the distilled water maintained at appropriate PH (3-4) using conc.HNO_3. This solution was stirred for 30 mins. To required amount of Na_2SO_4 as a dopant precursor (0.2 to 0.6 M) was dissolved in water. This dopant solution was then added to the above mixture solution and stirred vigorously for 8 hrs. This solution was then aged at room temperature for several hrs; the sols were transformed into gels, and washed with ethanol. The catalyst was dried at 80° C in the oven. Finally, the dried samples calcined at 500° C for 5 hrs, which resulted in S-TiO_2 nano particles. For comparison, pure TiO_2 was also prepared in the absence of Na_2SO_4 under similar approach.

Characterization

The X-ray diffraction patterns of the samples were recorded on a XPERT-PRO X-ray diffractometer with Cu-Kα radiation of wavelength 1.5406 A° in 2θ range from 20° to 70°. UV-visible spectrophotometer was using shimadzu UV-1650. Fourier transform infrared (FT-IR) spectroscopy measurement was recorded with AVATAR 330 FT-IR spectrometer in the range of 4000-500 cm^{-1}. SEM image was taken using JEOL, Model JSM 6390.

RESULTS AND DISCUSSION

X- ray diffraction studies

Fig.1 shows the X-ray diffraction (XRD) patterns of pure TiO_2 and S doped TiO_2. The diffractograms for TiO_2 are essentially equivalent, exhibiting peaks at 25.23, 38.9, 48.3, 55.28 and 62.88° that are consistent with the (1 0 1), (112), (2 0 0), (2 1 1) and (2 0 4) planes associated with tetragonal anatase (JCPDS No. 21-1272). There are four typical peaks with 2θ values of 27.38, 35.98, 41.18 and 54.18°, corresponding to the (1 1 0), (1 0 1), (1 1 1) and (2 1 1) crystal planes of the rutile phase (JCPDS No. 21-1276) [22], respectively. Compared with pure TiO_2, the (0.4M &0.6M) S-TiO_2 mainly shows the reflections corresponding to the rutile phase, and a trace amount of anatase phase. However, on further increasing the amount of the incorporation of S, the anatase phase gradually increases. It means that the ratio of anatase to rutile in the S-doped TiO_2 photocatalysts is strongly affected by the S dopant amount. In this study, some S peaks were observed. The peaks resulted from the reflection at 28.9, 33.48, 59.95° that was found for 0.4M & 0.6M sulfur doping, and it accords well with that in JCPDS 78-1889. The data obtained from the Scherer equation show increase in crystallite size (13 to 28 nm) with increase in sulfur content.

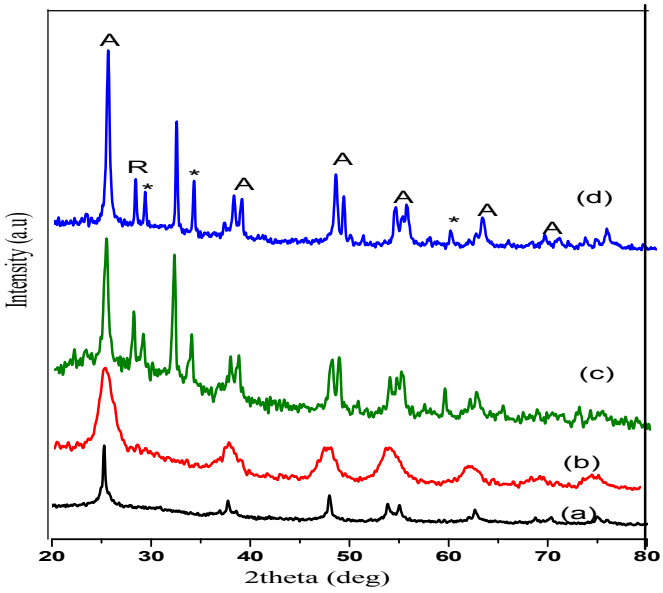

Fig 1 XRD Pattern of (a) Pure TiO_2 (b) (0.2M) S-TiO_2 (c) (0.4M) S-TiO_2 (d) (0.6M) S-TiO_2 A- Anatase R- Rutile *- Sulfur

Table 1 the 2θ Value, d-space, Average Crystal size (D), Different Concentration of S-TiO_2 (0.2, 0.4 and 0.6%) Nanoparticles Using XRD Spectra

Samples	2θ (°)	d-space (Å)	Average Crystalline size (D) nm
TiO_2	25.32	0.38	28
(0.2M) S-TiO_2	25.50	0.66	13
(0.4M) S-TiO_2	25.15	0.50	19
(0.6M) S-TiO_2	25.31	0.34	24

Table.1 shows the 2θ the full width at half maximum (FWHM) value, d-value, average crystal size (D) of different S concentrations (0.2, 0.4, 0.6 M) nano TiO_2. The particle size increases with increase in doping concentration.

Functional group Analysis (FT-IR)

FT-IR spectra of S-TiO_2 nanoparticles are shown in Fig.2. The peaks correspond to stretching vibrations of the O-H and bending vibrations of the adsorbed water molecules about 3350-3450 and 1620-1635cm^{-1}, respectively. These results strongly confirm the presence of hydroxyl ions in the structure of the samples [23]. The strong band in the range of 490-750 cm^{-1} is attributed to stretching vibrations of Ti-O-Ti bond [24, 25]. The peak observed in the range of 2356-2364 cm^{-1} was due to amine (NH) group stretching frequency [26]. The band at 2860 cm^{-1} was due to the C-H bonds of the organic compounds [27].

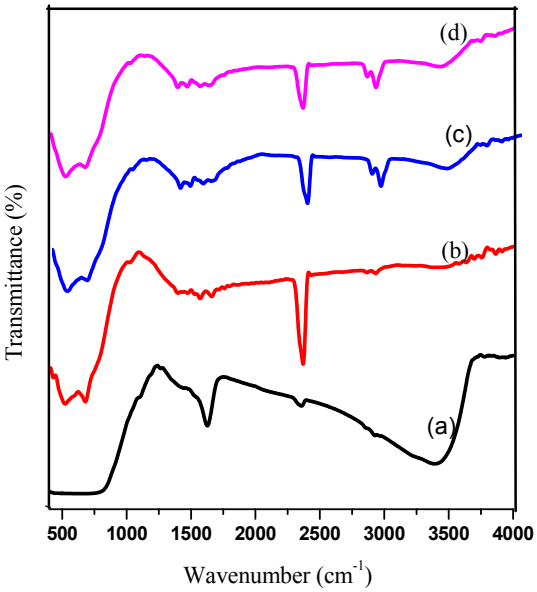

Fig 2 FT-IR Spectrum of (a) Pure TiO_2 (b) (0.2M) S-TiO_2 (c) (0.4M) S- TiO_2 (d) (0.6M) S-TiO_2

Surface Morphological Analysis

Scanning Electron Microscopy (SEM/EDS)

The morphology of the synthesized S doped TiO_2 nano particles measured by SEM is given in Fig.3. It can be seen that there were many irregular shape nanoparticles with various caves, which mainly resulted from the agglomeration of nano TiO_2. The images also show that the morphologies of TiO_2 samples correspond to their phase compositions and preparation conditions. The elemental composition of the obtained powder was determined using energy dispersive X-ray spectroscopic (EDS) analysis.

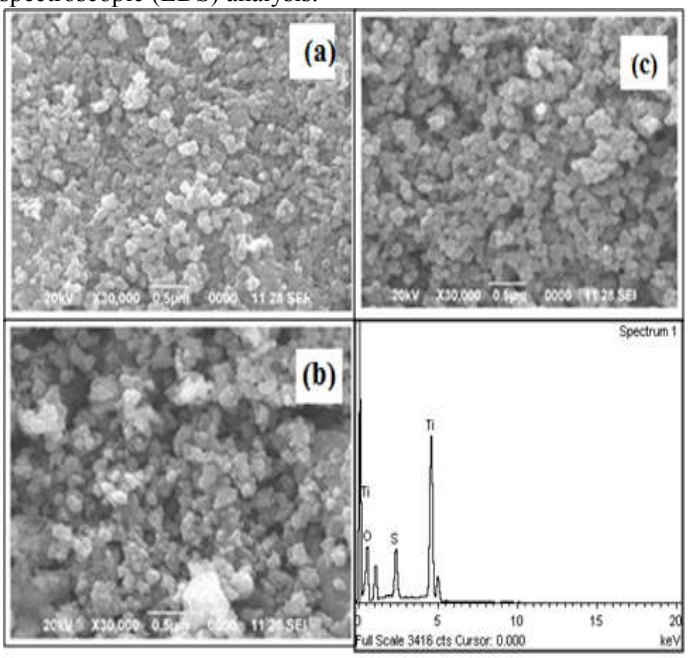

Fig 3 SEM/EDS Images of (a) (0.2M) S-TiO_2 (b) (0.4M) S-TiO_2, (c) (0.6M) S-TiO_2 (d) EDS Spectrum of (0.2M) -TiO_2

In the EDS spectrum, only characteristic peaks of Ti, S and O are observed which reveal that the obtained nanoparticles are composed of Ti, S and O in Fig.3 (d). This result also correlated with the results obtained by XRD analysis.

Optical Analysis

UV-Visible absorption spectrum

The optical properties and the energy band gap of pure and S-doped TiO_2 nanostructures were studied by UV-Visible absorption spectroscopy. The UV-Vis absorption spectra of the undoped and doped TiO_2 samples are shown in Fig.4. The corresponding absorption edge of pure TiO_2 and S-TiO_2 were 370 and 360, 365, 415 nm, respectively. Compared with the pure TiO_2, the doping samples showed a stronger absorption in the UV range and a slight shift to visible light range. While the absorption curve of the S-TiO_2 displayed a significant red shift compared with the undoped TiO_2 samples. According to the UV-Vis absorption spectra, the S-TiO_2 may have an excellent photocatalytic effect under the UV light region.

The band gap was calculated by using the plot of $(\alpha h\nu)^2$ vs. hν which is shown in Fig. 5. By assuming that TiO_2 has a direct type of transition

$$\alpha h\nu = A(h\nu - Eg)^{1/n}$$

where α, hν, A, Eg and n are the absorption coefficient, photon energy, proportionality constant, band gap and a constant respectively, where n decides the type of transition. The result shows that pure TiO_2 has a large band gap (3.4eV) and S doped TiO_2 has band gap energy which decreases with increase in concentration 3.33eV, 3.25eV, 2.93eV, respectively, by extrapolation of the linear portion of the absorption coefficient α to zero. The band gap energy decreases with the doping of sulfur ions, which allow the delay in recombination rate and enhance the photocatalytic activity.

In Table.2 shows the optical band gap energy decreases with increase in particle size, which can be attributed to the quantum size effect, improvement in morphological and crystallinity of the samples.

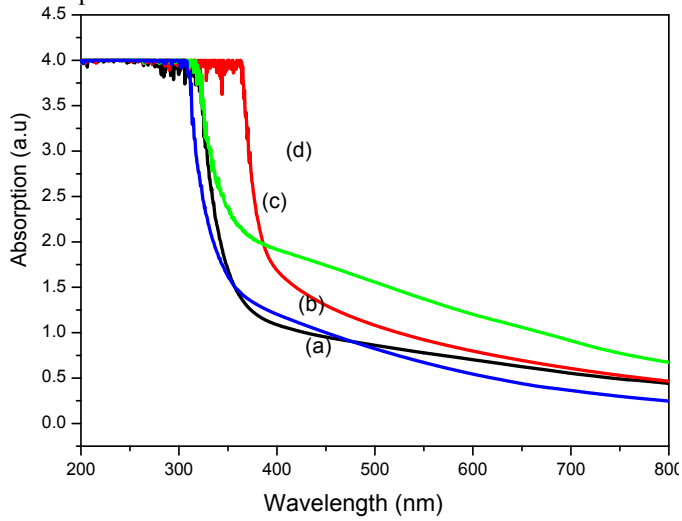

Fig 4 UV-Visible Spectra of (a) Pure TiO_2 (b) S- TiO_2 (0.2M) (c) S- TiO_2 (0.4M) (d) (0.6M) S- TiO_2

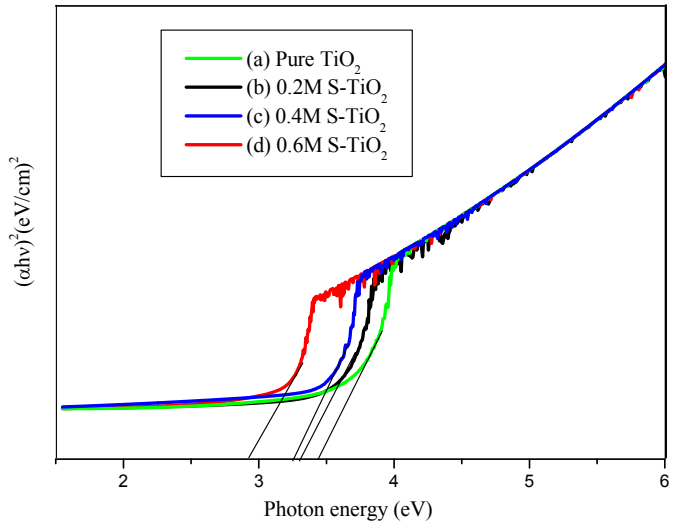

Fig 5 Optical Band Gap Diagram of (a) Pure TiO_2 (b) (0.2M) S-TiO_2 (c) (0.4M) S- TiO_2 (d) (0.6M) S-TiO_2

Table 2 Comparison of Eg and D Values of 0.2, 0.4, 0.6 M S-TiO_2 nanoparticles

S.No	Samples	Band gap Energy Eg (eV)	Crystallite Size (D) (nm)
1	Pure TiO2	3.4	28
2	(0.2 M) S-TiO_2	3.33	13
3	(0.4 M) S-TiO_2	3.25	19
4	(0.6 M) S-TiO_2	2.93	24

CONCLUSION

High quality undoped and S-doped TiO_2 nanocparticles were successfully synthesized by sol-gel method and investigated by different spectroscopy techniques which support the nanomaterials structure, morphology and optical properties of the prepared samples. From XRD results, compared with pure TiO_2, the 0.4M & 0.6M S-TiO_2 mainly shows the reflections corresponding to the rutile phase, and a trace amount of anatase phase. The 0.2M S-TiO_2 nanoparticles have smallest particle size. It is proposed that 0.2M S-TiO_2 doped gives better result, which is confirmed by the detailed XRD analysis and the derived structural parameters. From SEM images there were many irregular shape nanoparticles with various caves, which mainly resulted from the agglomeration of nanocrystaline TiO_2. The EDS result showed the elemental maping was performed by EDS analysis consisting of Ti, O, S. The presence of functional groups and the chemical bonding with S are confirmed by FTIR spectra. The PL spectrum of the TiO_2 shows a dominant emission band centered at 453 nm (2.74 eV), which is consistent with absorption measurement. This blue range emission peak is attributed to the near-band-edge emission. The low PL intensity of S-TiO_2 is ascribed to reduced recombination, which contributes to the photocatalytic activity.

References

1. A. Fujishima, K. Honda, Nature 238 (1972) 5551.
2. M.R. Hoffman, S.T. Martin, W. Choi, D.W. Bahnemann, Chem. Rev. 95 (1995) 69.
3. *T. Ohno et al. / Applied Catalysis A: General 265 (2004) 115-121* 121
4. L. Cao, F. Spiess, A. Huang, S.L. Suib, T.N. Obee, S.O. Hay, J.D. Freihaut, J. Phys. Chem. 103 (1999) 2912.
5. Endres, P. J.; Paunesku, T.; Vogt, S.; Meade, T. J.; Woloschak, G. E. J. Am. Chem. Soc. 2007, 129, 15760.
6. Fujishima, A.; Rao, T. N.; Tryk, D. A. J. Photochem. Photobiol., C 2000, 1, 1.
7. Sunada, K.; Kikuchi, Y.; Hashimoto, K.; Fujishima, A. Environ. Sci. Technol. 1998, 32, 726.
8. L. Gao, Nano-sized TiO2 Photocatalyst Materials and its Applications, Chemical Industry Press, 2002, pp. 104
9. Gaya U I, Abdullah A H. *J Photochem Photobiol C*, 2008, 9: 1
10. Nakata K, Fujishima A. *J Photochem Photobiol C*, 2012, 13: 169
11. Chen. S.S. Mao, Titanium dioxide nanomaterials synthesis, properties, modifications and applications, Chemical Reviews 107 (2007) 2891.
12. T.C. Dang, D.L. Pham, H.C. Le, V.H. Pham, TiO2/CdS nanocomposite films: Fabrication, characterization, electronic and optical properties, Advances in Natural Sciences: Nanoscience and Nanotechnology 01 (2010) 5002
13. P.N. Kapoor, S. Uma, S. Rodriguez, K.J. Klabunde, Aerogel processing of MTi2O5 (M = Mg, Mn, Fe, Co, Zn, Sn) compositions using single source precursors: synthesis, characterization and photocatalytic behavior, *J. Mol. Catal*. A 229 (2005) 145-150.
14. W.Y. Choi, A. Termin, M.R. Hoffmann, The role of metal ion dopants in quantum-sized TiO2: correlation between photoreactivity and charge carrier recombination dynamics, *J. Phys. Chem*. 98 (1994) 13669-13679.
15. X. Chen and S. S. Mao, *Chemical Reviews*, vol. 107, no. 7, pp. 2891-2959, 2007.
16. S. Livraghi, K. Elghniji, A. M. Czoska, M. C. Paganini, E. Giamello, and M. Ksibi, *Journal of Photochemistry and Photobiology A*, vol. 205, no. 2-3, pp. 93- 97, 2009.
17. J. G. Yu, W. G. Wang, B. Cheng, and B. L. Su, *Journal of Physical Chemistry C*, vol. 113, no. 16, pp. 6743-6750, 2009

18. K. Yang, Y. Dai, B. Huang, *J. Phys. Chem.* C 111 (2007) 18985e18994
19. Aarthi T, Madras G. Photocatalytic Degradation of Rhodamine Dyes with Nano-TiO2. Ind Eng Chem Res. 2007;46(1):7-14
20. VK, Suhas Ali I, Saini VK. Removal of Rhodamine B, Fast Green, and Methylene Blue from Wastewater Using Red Mud, an Aluminum Industry Waste. Ind Eng Chem Res. 2004;43(7):1740-1747.
21. Sarma J, Sarma A, Bhattacharyya, KG. Biosorption of Commercial Dyes on Azadirachta indica Leaf Powder: A Case Study with a Basic Dye Rhodamine B. Ind Eng Chem Res. 2008; 47:5433-5440.
22. Lu Q, Gao W, Du J, Zhou Li, Lian Y. Discovery of Environmental Rhodamine B Contamination in Paprika during the Vegetation Process. *J Agric Food Chem*, 2012; 60:4773−4778.
23. K. Tomita, V. Petrykin, M. Kobayashi, M. Shiro, M. Yoshimura, M. Kakihana, Angew. *Chem. Int. Ed*. 45 (2006) 2378.
24. J.A. Wang, R.L. Ballesteros, T. Lopez, A. Moreno, R. Gomez, O. Novaro, X. Bokhimi, *J.Phys. Chem*. B 105 (2001) 9692-9698.
25. S. Mucisc, M. Goti, M. Ivanda, S. Popovi, A. Turkovi, R. Trojko, A. Sekuli, K. Furi, Chemical and microstructural properties of TiO2 synthesized by sol-gel procedure, Mater. Sci. Eng. B47 (1997) 33-40
26. A. Manivannan, G. Glaspell, P. Dutta, Synthesis of nanocrystalline TiO2 particles and their structural characteristics, *J. Clust. Sci*. 19 (2008) 391-399.
27. G. Devanand Venkatasubbu a, S. Ramasamya,⇑, V. Ramakrishnan b, J. Kumara Folate targeted PEGylated titanium dioxide nanoparticles as a nanocarrier for targeted paclitaxel drug delivery Advanced Powder Technology 24, (2013) 947-954.
28. Santi Maensiri, Paveena Laokul, Jutharatana Klinkaewnarong A simple synthesis and room-temperature magnetic behavior of Co-doped anatase TiO2 nanoparticles *Journal of Magnetism and Magnetic Materials* 302 (2006) 448-453

How to cite this article:

Kavitha V.2019, Synthesis and Characterization of Sulfur Doped TiO^2 Nanoparticles for the Improved Photocatalytic Degradation of Rhodamine B by sol-gel Route. *Int J Recent Sci Res.* 10(07), pp.33763-33767.
DOI: http://dx.doi.org/10.24327/ijrsr.2019.1007.3744

****